Hindawi
International Journal of Photoenergy
Volume 2020, Article ID 3489218, 9 pages
https://doi.org/10.1155/2020/3489218

*Research Article*

# Obtaining and Characterization of $TiO_2$-GO Composites for Photocatalytic Applications

**D. K. Calvo Ramos,[1] M. Vega González,[2] R. A. Esparza Muñóz,[3] J. Santos Cruz,[1] F. J. De Moure-Flores,[1] and S. A. Mayén-Hernández[1]**

[1]*Facultad de Química, Posgrado en Ciencias de la Energía, Universidad Autónoma de Querétaro, 76010 Qro., Mexico*
[2]*Centro de Geociencias, Universidad Nacional Autónoma de México, Qro., Querétaro 76230, Mexico*
[3]*Centro de Física Aplicada y Tecnología Avanzada, Universidad Nacional Autónoma de México, Qro., Querétaro 76230, Mexico*

Correspondence should be addressed to S. A. Mayén-Hernández; sandra.mayen@uaq.edu.mx

Received 13 March 2019; Revised 19 May 2019; Accepted 28 May 2019; Published 5 August 2020

Academic Editor: P. Davide Cozzoli



Titanium dioxide (TD) and graphene oxide (GO) were synthesized by sol-gel and improved Hummers method, respectively. This study shows the results of the incorporation through four different conditions (sol-gel, sol-gel and ultrasonic, annealed, and UV radiation, C1 to C4, respectively). It was observed that a homogeneous incorporation of TD on sheets of GO was obtained satisfactorily. The composites of $TiO_2$/GO were characterized using different techniques such as X-ray diffraction (XRD), transmission electron microscopy (TEM), scanning electron microscopy (SEM), scanning transmission electron microscopy (STEM), energy dispersive X-ray spectroscopy (EDS), Raman spectroscopy, and infrared spectroscopy (IR). The photocatalytic activity of the composites was determined from the degradation of the dye azo tartrazine using UV and solar radiation. The best incorporation of TD nanoparticles on GO was obtained with condition C3 (thermal incorporation method) at a temperature of 65°C. This shows a uniformity in the size and shape of the TD as well as an excellent adherence to the sheet of GO. This addition is accomplished by ionic bonding in the presence of electrostatic Coulomb forces. The C3 composite degraded the tartrazine dye using UV radiation and sunlight. With the latter, the degradation time was three times faster than using UV light.

## 1. Introduction

Today, there is a wide variety of photocatalytic materials to degrade organic and inorganic contaminants. Within these materials, binary and ternary semiconductor oxides stand out. Among the most used and studied are ZnO [1–3], $Bi_2O_3$ [4, 5], various types of titanates [6–8], and $TiO_2$ [9, 10].

Titanium dioxide has three polyform phases: rutile, anatase, and brookite [1–3]. The two most important phases are anatase and rutile. The anatase phase has shown photocatalytic enhancement activity due to its physiochemical properties [4–9] such as a better specific area, a band gap (3.2 eV), and improved photocarrier lifetimes (~$10^{-9}$ s) [3]. TD is widely used as a photocatalyst due to its optical and electrical properties [10], its nontoxicity to the environment and humans [10–17], its high oxidative power [11, 16], its chemical and biological stability [10, 12, 14, 16, 17], its low production cost [10–16], and its higher photocatalytic activity [13, 17]. Because of these physiochemical properties, TD is considered to be a material with the potential for several applications.

However, the photocatalytic activity of this material is limited by the band gap (3.2 eV for anatase and 3.0 eV for rutile), which absorbs only in the ultraviolet region of the electromagnetic spectrum resulting in a low efficiency [18].

In recent decades, researchers have focused on doped TD to shift the absorption edge to the visible and red spectrum in order to reduce the times of photodegradation. The elements that have been used are Pt, Au, Pd, Rh, Ni, Cu, Ag, Co, Cr, Fe, Mo, V, and W [18–23]. The synergy with organic materials has also been investigated as in the case of the allotropes of carbon [24–27]. Currently, interest on graphene materials has increased due to their application in the photocatalysis area [28, 29]. The graphene oxide is defined as a blade of

graphene functionalized with hydroxyl and epoxy groups in the basal plane and carboxyls and carbonyls at the edges [30, 31]. The oxygen contained on the GO surface, as a functional group, is responsible for the incorporation of TD [27, 32, 33].

On the other hand, reduced graphene oxide (rGO) is defined as a sheet of functionalized graphene with only carboxyl and carbonyl groups at the edges [31]; rGO has shown advantageous enhancement of photocatalytic activity in a number of studies because it can promote charge separation and electron transfer, it can extend the light absorption range, and it possesses a high specific surface area. The incorporation of TD on the basal plane and edges of graphene oxide has been studied in the application to photocatalytic materials [18, 34–39] with very satisfactory results. This is because of the high capacity of the GO for capturing the TD photogenerated electrons, therefore interfering with recombination [35, 37, 40–42]. Different methods have been used to support the TD on GO: sol-gel [43], thermal (temperature range from 80°C to 120°C) [34, 44–46], and radiation (UV and Xenon lamps) [25, 42, 47, 48].

In this study, four different conditions were tested for incorporating TD into GO. The first used sol-gel synthesis to obtain TD that was incorporated directly into the GO. The second was by obtaining TD from sol-gel synthesis and incorporating it into the GO with the aid of ultrasound. The third was through the sonochemical synthesis of TD incorporated into the GO with the aid of thermal treatment. In the fourth test, the TD was obtained by sonochemical synthesis and incorporated into the GO with the aid of UV radiation and temperature. To determine the degree of incorporation ($TiO_2$/GO), the composites were characterized using X-ray diffraction (XRD), scanning electron microscopy (SEM), transmission electron microscopy (TEM), scanning transmission electron microscopy (STEM), Raman spectroscopy, and infrared spectroscopy (IR). To corroborate the increase in photocatalytic activity of the TD nanoparticles incorporated into the GO, photodegradation experiments of the azo tartrazine dye were conducted under UV radiation and solar light.

## 2. Experimental

*2.1. GO Synthesis.* GO was obtained using the improved Hummers method [25, 35, 42, 48, 49], which consisted of 360 mL of $H_2SO_4$, 40 mL of $H_3PO_4$, and 2 g of graphite powder mixed under vigorous stirring at room temperature for 2 hours. Then, 18 g of $KMnO_4$ and 800 mL of deionized water were slowly added, being careful to keep the temperature at 60°C using a recirculator. Finally, 15 mL of $H_2O_2$ (30%) was poured in. After 24 hours, the resulting solution was centrifuged and washed with deionized water and ethanol until a neutral pH was obtained. The solid obtained was dried at 65°C for 24 hours. Subsequently, the product was dispersed in water under ultrasound for 3 hours to obtain the exfoliated sheets.

*2.2. Sol-Gel TD Synthesis and Incorporation into GO (Composite C1).* The TD powder was obtained from 1 mole of titanium (IV) isopropoxide, 36 moles of ethanol, and 0.5 mole of hydrofluoric acid (HF). The acid was mixed with half the ethanol solution, and another half of ethanol was mixed with the isopropoxide. The first solution was poured slowly into the second with vigorous stirring. This synthesis was carried out in an inert atmosphere. No thermal treatment was applied after the synthesis. For the incorporation of the $TiO_2$/GO material, 20% *w*/*w* of GO was added to the sol-gel solution of TD and was allowed to precipitate. Subsequently, the solvent was evaporated at room temperature.

*2.3. Sol-Gel TD Synthesis and Ultrasound-Assisted Incorporation of GO (Composite C2).* To the sol-gel solution of TD, 20% *w*/*w* of GO was added. The solution was then placed in an ultrasonic bath for 2 hours and subsequently allowed to precipitate. The solvent was evaporated at room temperature. These samples did not undergo additional thermal treatment.

*2.4. Sonochemistry TD Synthesis and Thermally Assisted Incorporation of GO (Composite C3).* TD was synthesized by the sonochemistry technique using 50 mL of deionized water, a ratio of 1 mole of titanium (IV) isopropoxide for each 36 moles of ethanol, and 0.5 mole of HF. The water was mixed with half of the ethanol and the HF acid. The other half of the ethanol was poured with the isopropoxide (this mixture was prepared under an inert atmosphere). Then, the mixture was placed in an ultrasonic bath at 60°C for 3 hours. Under these conditions, TD was obtained in the anatase phase with a nanometric size on the order of 50 nm. For the incorporation of GO, 20% *w*/*w* of the GO, deionized water, and ethanol in a 1 : 1 (*v*/*v*) ratio were added. The solution was immediately placed in an ultrasound bath for 2 hours in order to disperse the particles. After that, the dispersion was stirred and heated at 65°C for 24 hours.

*2.5. Sonochemistry TD Synthesis and UV Radiation-Assisted Incorporation of GO (Composite C4).* TD was obtained by sonochemistry methodology, and then, 20% *w*/*w* of GO was added to a deionized water and ethanol solution (1 : 1 *v*/*v*). The solution was left in an ultrasonic bath for 2 hours in order to disperse the particles. After that, the solution was stirred for 24 hours at a constant temperature of 65°C under the radiation of a germicidal lamp model PLS 9W (UV 254 nm).

*2.6. Photodegradation of the Tartrazine Dye.* The photodegradation experiments were conducted using two procedures.

(1) Under the influence of a germicidal lamp (UV 254 nm) in the presence of the four separate composites (C1, C2, C3, and C4), 400 mL of the tartrazine solution was poured into a concentration of $7 \times 10^{-5}$ mol · $L^{-1}$ and 0.2 g of composite. The experiments were kept in constant agitation, obtaining aliquots at 10 min intervals. The residual absorbency of the tartrazine was measured at 190 to 550 nm

(2) Using solar radiation with turbulent recirculation of the tartrazine solution in the presence of the four

separate composites (C1, C2, C3, and C4), 3 L of the tartrazine solution was poured into a concentration of $7 \times 10^{-5}$ mol · $L^{-1}$ and 1.5 g of composite. The recirculation was kept constant with the aid of a pump with a 20 L per minute capacity. The aliquots were obtained at 30 min intervals, and the residual absorbency of the tartrazine was measured at 190 to 550 nm

The remnant concentration of the tartrazine solution was measured in a UV-Vis Thermo Scientific Genesys 10S spectrophotometer.

*2.7. Characterization.* The samples of the four incorporations were characterized by different techniques using the following: X-ray diffractometer (XRD) in a Rigaku Miniflex using Cu K$\alpha$ radiation ($\lambda = 1.5418$ Å) with a source at 30 kV, transmission electronic microscope (TEM) JEOL model JEM-1010 with a source at 80 kV, scanning electron microscope (SEM) Hitachi model TM 1000 with a backscattered detector, scanning electron microscope (HR-SEM) coupled to an EDS probe and Hitachi STEM mode model SU8230, Thermo Scientific Raman spectroscopy model DXR2, and infrared spectroscopy (IR) Bruker model Tensor 27.

## 3. Results and Discussion

*3.1. Characterization of the C1, C2, C3, and C4 Samples.* Figure 1 shows the XRD patterns of the $TiO_2$/GO composites, the TD nanoparticles, and the GO sheets. For the samples C1 and C2, the material is very little crystalline. From the Scherrer-Debye equation, the crystal size of the TD is 5 nm for samples C3 and C4. In these samples, the characteristic plans of the anatase phase are observed at 25.2° (101), 37.6° (004), 47.7° (200), 54.1° (105), 62.3° (213), 69.4° (116), and 74.8° (215). None of the four diffraction patterns presents the peak characteristic of the GO ($2\theta = 12.3°$), corresponding to the crystallographic plane (001), indicating that in the process of incorporation the sheets of GO were completely exfoliated and these are covered by TD nanoparticles.

This addition takes place by ionic bonding in the presence of an electrostatic Coulomb force. In a contaminant degradation process, the greater the homogeneity and the incorporation of nanoparticles of TD in the GO sheets, the greater the predominance of the photocatalytic process on the possible adsorption process. The adsorption can occur due to the high specific surface of the GO [45, 50].

Figure 2 shows the TEM images of the compounds and TD powder. In samples C1 and C2, the TD particles are dispersed in a less homogeneous manner in the GO than in C3 and C4. The homogeneity of the composite material is important to obtain an efficient transfer of electrons captured from the TD [41, 43], reducing the recombination times and increasing the photocatalytic activity. This superposition of TD nanoparticles observed in the TEM images corroborates the XRD results, where it is not possible to observe the characteristic GO peak ($2\theta = 12.3°$) with the crystalline plane (001) due to the agglomeration of TD in the exfoliation GO

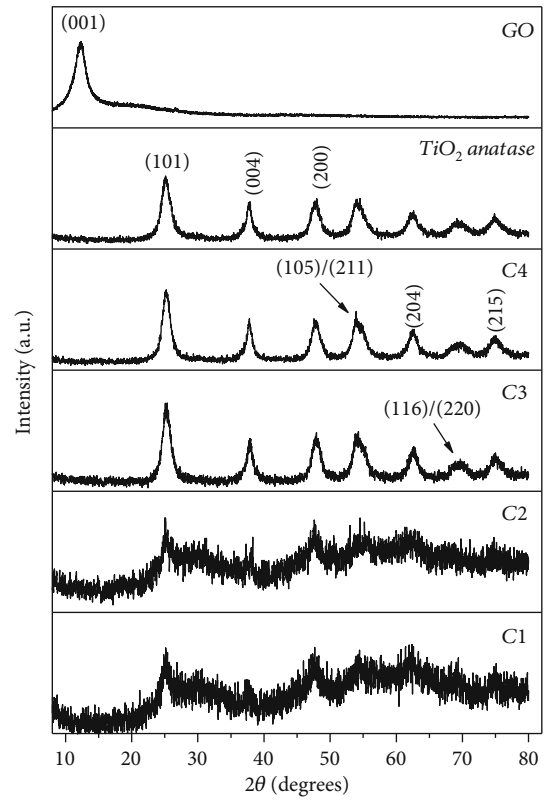


Figure 1: XRD diffraction patterns of GO, TD, and the composite materials C1, C2, C3, and C4.

sheets. Additionally, in these images, the size of the TD nanoparticles (>20 nm) is shown.

To observe with greater detail the incorporation of the TD nanoparticles on the surface of the GO laminae clusters, an incorporation with a minimal quantity of TD was realized (C3), and this was analyzed by HR-SEM in STEM mode. As shown in Figure 3, the sample was taken in a bright field. It can be observed how the TD nanoparticles adhere to the GO sheet. This union takes place by electrostatic attraction between TD and the surface of the GO sheets. The TD becomes incorporated onto the GO sheets until they are covered; this has also been observed by other investigators [51, 52]. In contrast to what has been reported in the literature, the incorporation for composite C3 was obtained at a temperature of 65°C, the lowest reported to date. The size of the GO sheets was 2 $\mu$m on average.

Elemental analysis by EDS was performed to corroborate the incorporation of TD on the surface of the GO sheets. The images were taken with the detector of secondary electrons (SE) and, by mapping EDS, finding representative elements of the sample: carbon, titanium, and oxygen (Figure 4). With this analysis, the presence of TD is confirmed on the GO sheets, and the oxygen found could be attributed to the functional groups present in the GO. Additionally, Figures 4(a)–4(f) show EDS elemental analysis for the composite S3 showing different elements and colors: GO sheet with TD nanoparticles, perspective image; identification of the carbon in green; titanium present on the GO in red; oxygen in blue; elemental identification of Ti, C, and O; and elemental

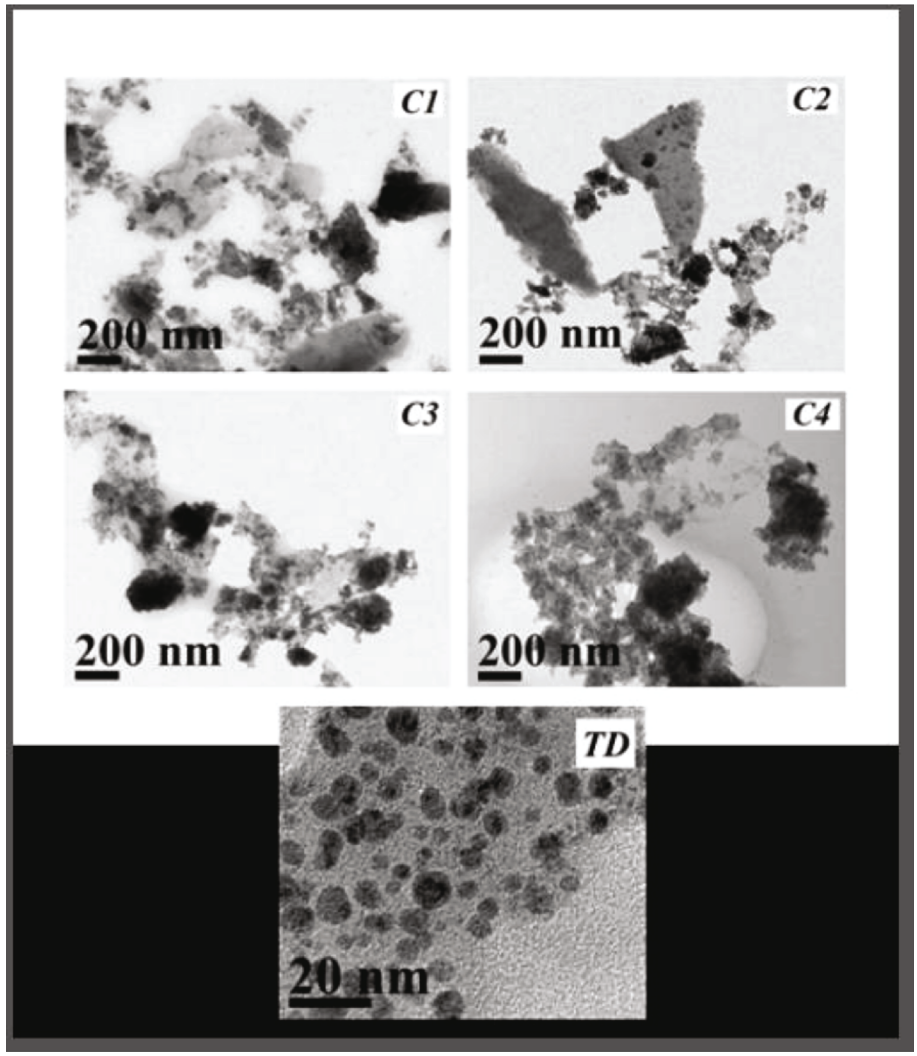


Figure 2: TEM images of composite materials C1 to C4 and nanoparticles of TD.

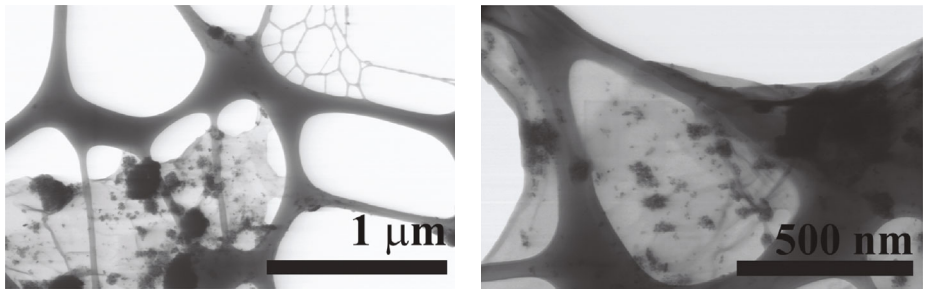


(a) (b)

Figure 3: STEM bright-field images.

identification of Ti and O. The EDS analysis corresponds to the stoichiometry of $TiO_2$.

The characteristic bands of TD and those of GO were found by Raman spectroscopy in the four syntheses, as shown in Figure 5. For TD, four modes of the anatase phase are observed: two modes of $E_g$ at 156 and 637 $cm^{-1}$, one mode of $B_{1g}$ at 402 $cm^{-1}$, and one mode of $A_{1g}$ at 512 $cm^{-1}$, corresponding to that reported in the literature [50, 51]. For the GO, three modes were identified: the band $D$ at 1336 $cm^{-1}$, attributed to the defects and the disorder of the sheet; $G$ mode at 1603 $cm^{-1}$ assigned to the $sp^2$ hybridization plane of the vibrations of the carbon atoms; and the 2$D$ mode at

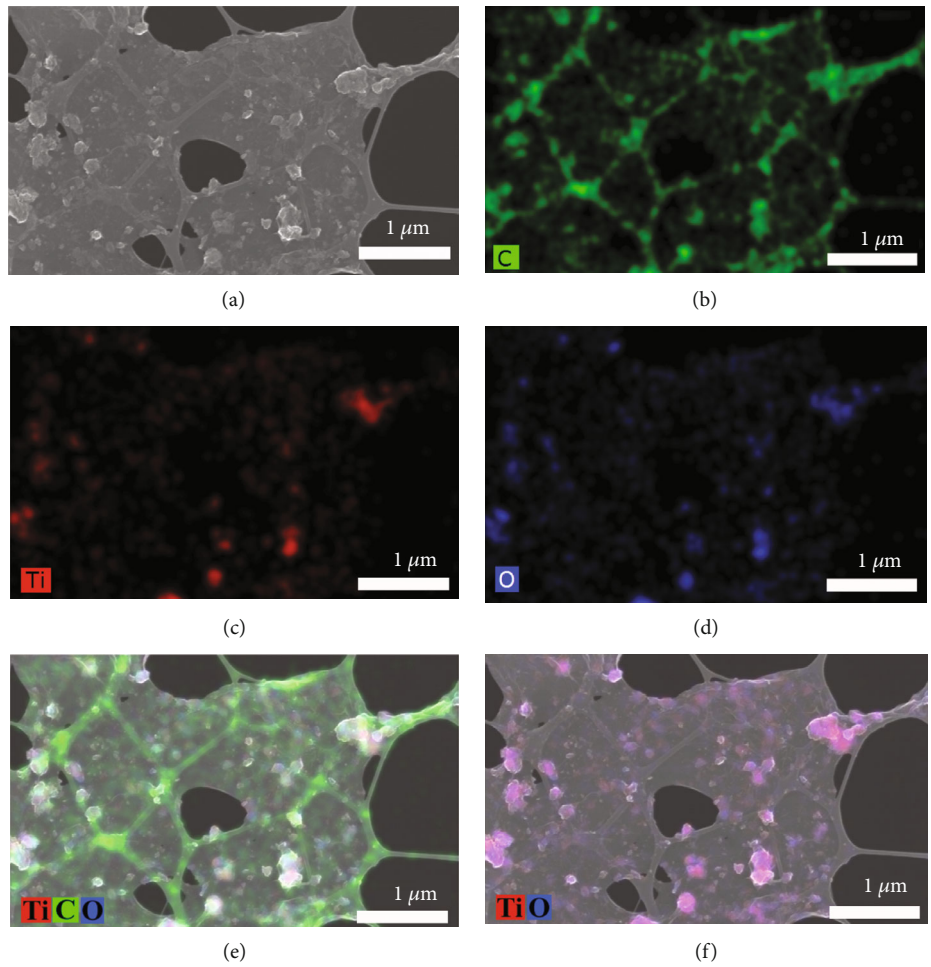


FIGURE 4: EDS elemental analysis for C3 compound. Different elements is displayed and color, respectively a)GO sheet with TD nanoparticles, b)identification of carbon as a green color, c) titanium present in the GO as a red color,(d) oxygen as a blue (e) identification elemental Ti, C and O, f) Ti and elemental identification O.

2936 $cm^{-1}$, with a low intensity which is related to the Raman band second-order effect of phonons [46, 52–55]. The intensity of the GO bands (*D*, *G*, and 2*D*) is related to the homogeneity and the incorporation of the composites, as is observed in Figure 6. The composites C3 and C4 show the lowest intensities of the GO bands, but they are present in the material. This can be observed in the increase added to each plot.

Figure 6 shows the IR spectra of the four composite syntheses of the $TiO_2$/GO material. The band at 3318 $cm^{-1}$ and 1632 $cm^{-1}$ is attributed to the stretching of the hydroxyl groups ($H_2O$, C-OH), at 1365 $cm^{-1}$ to the carboxyl group (-COOH), at 1632 $cm^{-1}$ confirms vibrational stretch (C=C), at 1208 $cm^{-1}$ to the epoxy functional groups (-C-O-C-), at 1105 $cm^{-1}$ to the alkoxy functional groups (RO-), at 1082 $cm^{-1}$ attributed to vibration (Ti-O-C), and at the 900 $cm^{-1}$ to 500 $cm^{-1}$ attributed to vibration titanium-oxygen (Ti-O and Ti-O-Ti) [46, 48, 53, 56]. All of these vibrational modes show a strong chemical interaction between the TD and GO in the synthesis of the composite.

*3.2. Photocatalytic Activity.* The photocatalytic activity of the four composites (C1, C2, C3, and C4) was evaluated through the degradation of the tartrazine dye. Figure 7 shows the degradation curves of the dye in the presence of UV radiation at a normalized concentration as a function of time. It is observed that at 60 minutes the TD powder degraded almost 1% of the dye, very similar to the photolysis results and indicating that the presence of TD is not enough to achieve a degradation of this dye despite what has been reported in the literature [56].

With respect to the results of the composites, we can observe that with C1 and C2 a degradation close to 3% was achieved. With C3, a degradation of more than 23% was achieved, and the tartrazine degraded 10% with C4. These results are consistent with the characterization realized for the four composites, where C3 demonstrated having a greater homogeneity in the incorporation of the two materials ($TiO_2$/GO).

We conducted two control experiments: adsorption and photolysis. Regarding the first adsorption percentage was ~1%; this percentage confirmed that the process is actually being carried out which is photocatalysis. Regarding the second control experiment, it is confirmed that the UV radiation has little influence on the degradation of the dye.

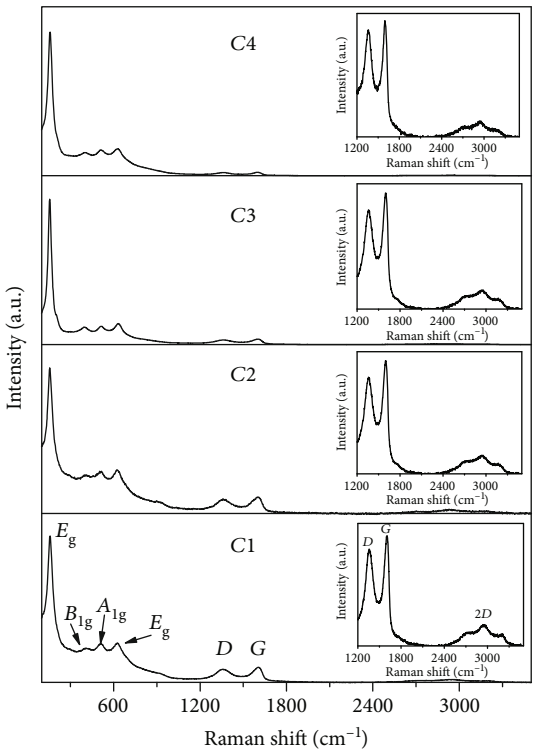


Figure 5: Raman spectra of the four compounds to check the active vibrational modes of the composite $TiO_2$/GO.

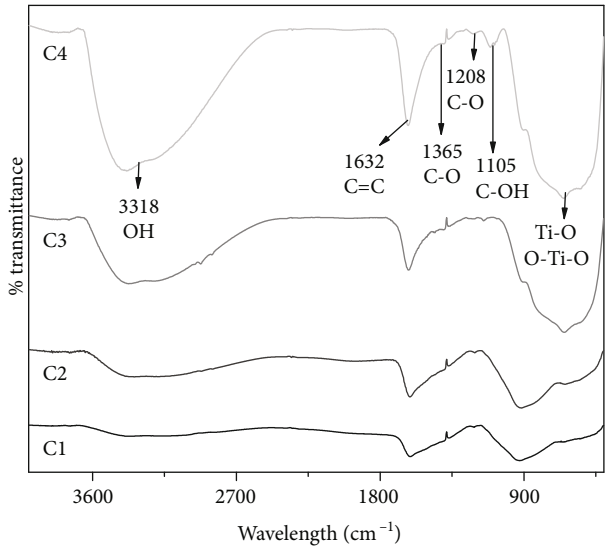


Figure 6: IR spectra of the four compounds for the presence of functional group characteristics of GO.

The increase in the percentage of degradation is due to the incorporation of GO sheets; the function of this material is to be an electron acceptor recombination from $TiO_2$. This process influences time photocatalysis degradation.

Figure 8 shows the degradation curves of the dye normalized as a function of time and with solar radiation. The experiments were realized under the various solar conditions that are present in the day, with better results in comparison with

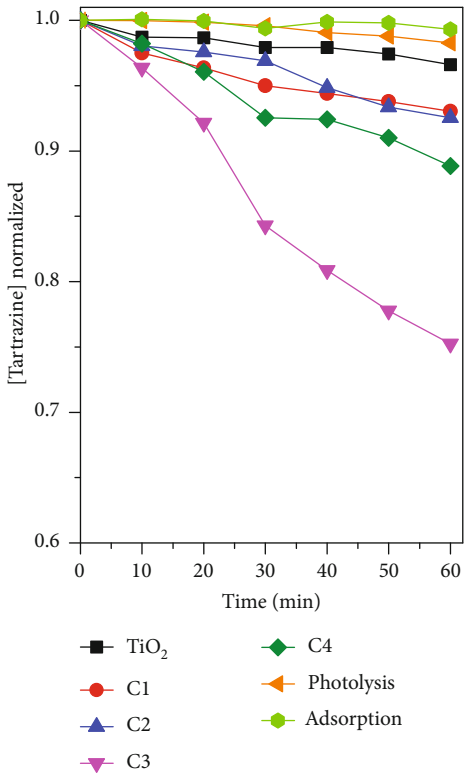


Figure 7: Tartrazine azo dye degradation curves in the presence of UV lamp.

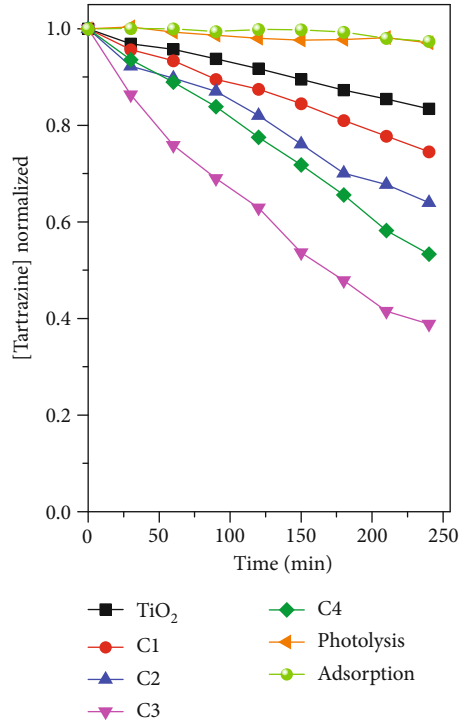


Figure 8: Degradation curves of azo tartrazine dye from solar radiation.

the experiments using UV radiation. For the photolysis, no change was observed in the initial concentration of tartrazine. For the TD powder, a degradation of 15% was obtained, 25% for C1, 35% for C2, 63% for C3, and 45% for C4; all the experiments had a duration of 240 min. These results are related to the UV radiation experiments, where it is observed that the best degradation results are obtained for the C3 composite.

With the C3 sample and the solar radiation, the degradation of the dye tripled, demonstrating that the incorporation of TD and GO increases the photocatalytic activity of the TD. Also, it results in a degradation of the azo dye without a need to incorporate donor species to decompose the molecule.

## 4. Conclusions

The characterization of the different $TiO_2$/GO composites demonstrated that a material with a greater degree of homogeneity of TD on the GO sheets was obtained with incorporation conditions of C3 (ultrasound and 65°C temperature). It should be pointed out that the temperature that allowed this incorporation is the lowest reported, as far as we know. It was possible to corroborate the results of the characterization with photodegradation experiments of the tartrazine. A greater degradation of the dye was found with the C3 composite. A degradation of 20% was obtained under UV radiation conditions and 63% with solar radiation. This demonstrated that the incorporation with GO increases the photocatalytic activity of pure TD. The heterogeneous photocatalysis with $TiO_2$/GO composites demonstrated it to be viable for the degradation of azo dyes, which has been reported to be difficult to degrade using solar light.

## Data Availability

No data were used to support this study.

## Conflicts of Interest

The authors declare that there is no conflict of interest regarding the publication of this paper.

## Acknowledgments

The team thanks the academic technician Ing. Biochemist Ma. Lourdes Tirado Palma, Institute of Neurobiology, UNAM, for the support on the TEM measurements.

## References

[1] H. Chen, Y. Shao, Z. Xu et al., "Effective catalytic reduction of Cr (VI) over $TiO_2$ nanotube supported Pd catalysts," *Applied Catalysis B: Environmental*, vol. 105, no. 3-4, pp. 255–262, 2011.

[2] C.-C. Wang, X.-D. Du, J. Li, X.-X. Guo, P. Wang, and J. Zhang, "Photocatalytic Cr (VI) reduction in metal-organic frameworks: a mini-review," *Applied Catalysis B: Environmental*, vol. 193, pp. 198–216, 2016.

[3] R. Kaplan, B. Erjavec, G. Dražić, J. Grdadolnik, and A. Pintar, "Simple synthesis of anatase/rutile/brookite $TiO_2$ nanocomposite with superior mineralization potential for photocatalytic degradation of water pollutants," *Applied Catalysis B: Environmental*, vol. 181, pp. 465–474, 2016.

[4] S. Bang, M. Patel, L. Lippincott, and X. Meng, "Removal of arsenic from groundwater by granular titanium dioxide adsorbent," *Chemosphere*, vol. 60, no. 3, pp. 389–397, 2005.

[5] R. Fagan, D. W. Synnott, D. E. McCormack, and S. C. Pillai, "An effective method for the preparation of high temperature stable anatase $TiO_2$ photocatalysts," *Applied Surface Science*, vol. 371, pp. 447–452, 2016.

[6] W. Hu, Y. Yu, H. Chen et al., "Synthesis and chemical modifications of in-situ grown anatase $TiO_2$ microspheres with isotropically exposed {0 0 1} facets for superhydrophobic and self-cleaning properties," *Applied Surface Science*, vol. 357, pp. 2022–2027, 2015.

[7] A. N. Banerjee, N. Hamnabard, and S. W. Joo, "A comparative study of the effect of Pd-doping on the structural, optical, and photocatalytic properties of sol–gel derived anatase $TiO_2$ nanoparticles," *Ceramics International*, vol. 42, no. 10, pp. 12010–12026, 2016.

[8] Y. Chen, Y. Xu, S. Jiao et al., "Synthesis of blue anatase $TiO_2$ nanoplates with {001} facets and in situ noble metal anchoring," *Dyes and Pigments*, vol. 129, pp. 191–198, 2016.

[9] C. L. Lai, H. L. Huang, J. H. Shen, K. K. Wang, and D. Gan, "The formation of anatase $TiO_2$ from TiO nanocrystals in sol-gel process," *Ceramics International*, vol. 41, no. 3, pp. 5041–5048, 2015.

[10] M. I. Litter and N. Quici, "New advances in heterogeneous photocatalysis for treatment of toxic metals and arsenic," *Nanomaterials for Environmental Protection*, vol. 97811, pp. 143–167, 2014.

[11] S. W. Zhou, P. Peng, J. Liu, Y. H. Tang, B. Meng, and Y. X. Peng, "Investigation on the electronic structures and optical performances of Si-S codoped anatase $TiO_2$ by first-principles calculation," *Physics Letters A*, vol. 380, no. 16, pp. 1462–1468, 2016.

[12] A. Sasani, A. Baktash, K. Mirabbaszadeh, and B. Khoshnevisan, "Structural and electronic properties of Mg and Mg-Nb co-doped $TiO_2$ (101) anatase surface," *Applied Surface Science*, vol. 384, pp. 298–303, 2016.

[13] C. Xie, S. Yang, B. Li et al., "C-doped mesoporous anatase $TiO_2$ comprising 10 nm crystallites," *Journal of Colloid and Interface Science*, vol. 476, pp. 1–8, 2016.

[14] D. Nabi, I. Aslam, and I. A. Qazi, "Evaluation of the adsorption potential of titanium dioxide nanoparticles for arsenic removal," *Journal of Environmental Sciences*, vol. 21, no. 3, pp. 402–408, 2009.

[15] D. Hazarika and N. Karak, "Photocatalytic degradation of organic contaminants under solar light using carbon dot/titanium dioxide nanohybrid, obtained through a facile approach," *Applied Surface Science*, vol. 376, pp. 276–285, 2016.

[16] Y. C. Cao, Z. Fu, W. Wei et al., "Reduced graphene oxide supported titanium dioxide nanomaterials for the photocatalysis with long cycling life," *Applied Surface Science*, vol. 355, pp. 1289–1294, 2015.

[17] T. T. Pham, C. Nguyen-Huy, and E. W. Shin, "Facile one-pot synthesis of nickel-incorporated titanium dioxide/graphene oxide composites: enhancement of photodegradation under visible-irradiation," *Applied Surface Science*, vol. 377, pp. 301–310, 2016.

[18] N. Prabhakarrao, M. R. Chandra, and T. S. Rao, "Synthesis of Zr doped $TiO_2$/reduced graphene oxide (rGO) nanocomposite material for efficient photocatalytic degradation of eosin blue dye under visible light irradiation," *Journal of Alloys and Compounds*, vol. 694, pp. 596–606, 2017.

[19] A. H. Al-Muhtaseb and M. Khraisheh, "Photocatalytic removal of phenol from refinery wastewater: catalytic activity of Cu-doped titanium dioxide," *Journal of Water Process Engineering*, vol. 8, pp. 82–90, 2015.

[20] C. Chambers, S. B. Stewart, B. Su, H. F. Jenkinson, J. R. Sandy, and A. J. Ireland, "Silver doped titanium dioxide nanoparticles as antimicrobial additives to dental polymers," *Dental Materials*, vol. 33, no. 3, pp. e115–e123, 2017.

[21] J. A. Torres-Luna, N. R. Sanabria, and J. G. Carriazo, "Powders of iron(III)-doped titanium dioxide obtained by direct way from a natural ilmenite," *Powder Technology*, vol. 302, pp. 254–260, 2016.

[22] W. Zhang, Y. Liu, X. Pei, and X. Chen, "Effects of indium doping on properties of xIn-0.1%Gd-$TiO_2$ photocatalyst synthesized by sol-gel method," *Journal of Physics and Chemistry of Solids*, vol. 104, pp. 45–51, 2017.

[23] M. Abdullah and S. K. Kamarudin, "Titanium dioxide nanotubes (TNT) in energy and environmental applications: an overview," *Renewable and Sustainable Energy Reviews*, vol. 76, pp. 212–225, 2017.

[24] E. Kusiak-Nejman, A. Wanag, L. Kowalczyk et al., "Graphene oxide-$TiO_2$ and reduced graphene oxide-$TiO_2$ nanocomposites: insight in charge-carrier lifetime measurements," *Catalysis Today*, vol. 287, pp. 189–195, 2017.

[25] P. Fernández-Ibáñez, M. I. Polo-López, S. Malato et al., "Solar photocatalytic disinfection of water using titanium dioxide graphene composites," *Chemical Engineering Journal*, vol. 261, pp. 36–44, 2015.

[26] J. Jing, Y. Zhang, W. Li, and W. W. Yu, "Visible light driven photodegradation of quinoline over $TiO_2$/graphene oxide nanocomposites," *Journal of Catalysis*, vol. 316, pp. 174–181, 2014.

[27] H. Raghubanshi, S. M. Ngobeni, A. O. Osikoya et al., "Synthesis of graphene oxide and its application for the adsorption of Pb +2 from aqueous solution," *Journal of Industrial and Engineering Chemistry*, vol. 47, pp. 169–178, 2017.

[28] C. Han, N. Zhang, and Y. J. Xu, "Structural diversity of graphene materials and their multifarious roles in heterogeneous photocatalysis," *Nano Today*, vol. 11, no. 3, pp. 351–372, 2016.

[29] H. He, J. Klinowski, M. Forster, and A. Lerf, "A new structural model for graphite oxide," *Chemical Physics Letters*, vol. 287, no. 1-2, pp. 53–56, 1998.

[30] C. K. Chua and M. Pumera, "Chemical reduction of graphene oxide: a synthetic chemistry viewpoint," *Chemical Society Reviews*, vol. 43, no. 1, pp. 291–312, 2014.

[31] D. W. Boukhvalov and M. I. Katsnelson, "Modeling of Graphite Oxide," *Journal of the American Chemical Society*, vol. 130, no. 32, pp. 10697–10701, 2008.

[32] S. Gilje, S. Han, M. Wang, K. L. Wang, and R. B. Kaner, "A chemical route to graphene for device applications," *Nano Letters*, vol. 7, no. 11, pp. 3394–3398, 2007.

[33] L. L. Tan, W. J. Ong, S. P. Chai, and A. R. Mohamed, "Photocatalytic reduction of $_{CO\ 2}$ with H 2 O over graphene oxide-supported oxygen-rich $_{TiO\ 2}$ hybrid photocatalyst under visible light irradiation: process and kinetic studies," *Chemical Engineering Journal*, vol. 308, pp. 248–255, 2017.

[34] M. Hamandi, G. Berhault, C. Guillard, and H. Kochkar, "Reduced graphene oxide/$TiO_2$ nanotube composites for formic acid photodegradation," *Applied Catalysis B: Environmental*, vol. 209, pp. 203–213, 2017.

[35] W. K. Jo, S. Kumar, M. A. Isaacs, A. F. Lee, and S. Karthikeyan, "Cobalt promoted $TiO_2$/GO for the photocatalytic degradation of oxytetracycline and Congo red," *Applied Catalysis B: Environmental*, vol. 201, pp. 159–168, 2017.

[36] H. H. Mohamed, "Biphasic $TiO_2$ microspheres/reduced graphene oxide for effective simultaneous photocatalytic reduction and oxidation processes," *Applied Catalysis A: General*, vol. 541, pp. 25–34, 2017.

[37] A. W. Morawski, E. Kusiak-Nejman, A. Wanag et al., "Photocatalytic degradation of acetic acid in the presence of visible light-active $TiO_2$-reduced graphene oxide photocatalysts," *Catalysis Today*, vol. 280, pp. 108–113, 2017.

[38] Y. Li, W. Cui, L. Liu et al., "Removal of Cr (VI) by 3D $TiO_2$-graphene hydrogel via adsorption enriched with photocatalytic reduction," *Applied Catalysis B: Environmental*, vol. 199, pp. 412–423, 2016.

[39] E. Kusiak-Nejman, A. Wanag, Ł. Kowalczyk et al., "Graphene $_{oxide\text{-}TiO\ 2}$ and reduced graphene $_{oxide\text{-}TiO\ 2}$ nanocomposites: insight in charge-carrier lifetime measurements," *Catalysis Today*, vol. 287, pp. 189–195, 2017.

[40] P. Wang, S. Zhan, Y. Xia, S. Ma, Q. Zhou, and Y. Li, "The fundamental role and mechanism of reduced graphene oxide in rGO/Pt-$TiO_2$ nanocomposite for high-performance photocatalytic water splitting," *Applied Catalysis B: Environmental*, vol. 207, pp. 335–346, 2017.

[41] M. Sohail, H. Xue, Q. Jiao et al., "Synthesis of well-dispersed $TiO_2$ reduced graphene oxide (rGO) nanocomposites and their photocatalytic properties," *Materials Research Bulletin*, vol. 90, pp. 125–130, 2017.

[42] M. Faraldos and A. Bahamonde, "Environmental applications of titania-graphene photocatalysts," *Catalysis Today*, vol. 285, pp. 13–28, 2017.

[43] Y. Zhu, Y. Wanh, W. Yao, R. Zong, and Y. Zhu, "New insights into the relationship between photocatalytic activity and TiO2-GR composites," *RSC Advances*, vol. 5, pp. 29201–29208, 2017.

[44] Y. Zhang, Z.-R. Tang, X. Fu, and Y.-J. Xu, "$TiO_2$–graphene nanocomposites for gas-phase photocatalytic degradation of volatile aromatic pollutant: is $TiO_2$–graphene truly different from other $TiO_2$–carbon composite materials?," *ACS Nano*, vol. 4, no. 12, pp. 7303–7314, 2010.

[45] X. Pan, Y. Zhao, S. Liu, C. L. Korzeniewski, S. Wang, and Z. Fan, "Comparing Graphene-TiO2Nanowire and Graphene-TiO2Nanoparticle composite photocatalysts," *ACS Applied Materials & Interfaces*, vol. 4, no. 8, pp. 3944–3950, 2012.

[46] O. Akhavan, M. Abdolahad, A. Esfandiar, and M. Mohatashamifar, "Photodegradation of graphene oxide sheets by TiO2Nanoparticles after a photocatalytic reduction," *Journal of Physical Chemistry C*, vol. 114, no. 30, pp. 12955–12959, 2010.

[47] H. M. Yadav and J. S. Kim, "Solvothermal synthesis of anatase $TiO_2$-graphene oxide nanocomposites and their photocatalytic performance," *Journal of Alloys and Compounds*, vol. 688, pp. 123–129, 2016.

[48] J. Bahadur and K. Pal, "Structural and magnetic properties of reduced graphene $_{oxide\text{-}TiO\ 2}$ nanoflower composite," *Physica*

*E: Low-dimensional Systems and Nanostructures*, vol. 90, pp. 98–103, 2017.

[49] J. L. Aguilar Salinas, J. R. Pacheco Aguilar, S. A. Mayén Hernández, and J. Santos Cruz, "Bactericidal activity of $TiO_2$ on cells of Pseudomonas aeruginosa ATCC 27853," *International Journal of Photoenergy*, vol. 2013, 7 pages, 2013.

[50] W. F. Zhang, Y. L. He, M. S. Zhang, Z. Yin, and Q. Chen, "Raman scattering study on anatase TiO2nanocrystals," *Journal of Physics D: Applied Physics*, vol. 33, no. 8, pp. 912–916, 2000.

[51] V. Gupta, N. Sharma, U. Singh, M. Arif, and A. Singh, "Higher oxidation level in graphene oxide," *Optik*, vol. 143, pp. 115–124, 2017.

[52] D. Liang, C. Cui, H. Hu et al., "One-step hydrothermal synthesis of anatase $TiO_2$/reduced graphene oxide nanocomposites with enhanced photocatalytic activity," *Journal of Alloys and Compounds*, vol. 582, pp. 236–240, 2014.

[53] C. Xiang, M. Li, M. Zhi, A. Manivannan, and N. Wu, "Reduced graphene oxide/titanium dioxide composites for supercapacitor electrodes: shape and coupling effects," *Journal of Materials Chemistry*, vol. 22, no. 36, p. 19161, 2012.

[54] M. W. Iqbal, A. K. Singh, M. Z. Iqbal, and J. Eom, "Raman fingerprint of doping due to metal adsorbates on graphene," *Journal of Physics. Condensed Matter*, vol. 24, no. 33, p. 335301, 2012.

[55] S. Liu, H. Sun, S. Liu, and S. Wang, "Graphene facilitated visible light photodegradation of methylene blue over titanium dioxide photocatalysts," *Chemical Engineering Journal*, vol. 214, pp. 298–303, 2013.

[56] V. K. Gupta, R. Jain, A. Nayak, S. Agarwal, and M. Shrivastava, "Removal of the hazardous dye-tartrazine by photodegradation on titanium dioxide surface," *Materials Science and Engineering: C*, vol. 31, no. 5, pp. 1062–1067, 2011.